Reprinted from *Proceedings of the 20th Int'l Conference on Coastal Engineering*, Vol. I (Billy L. Edge, Ed.), 1986, ASCE, pp. 737-751.

CHAPTER 56

TROPICAL CYCLONE GENERATED CURRENTS

by

Y. Peter Sheng, M.ASCE[1], and Sherman S. Chiu[2]

ABSTRACT

AXCP data obtained during Hurricane Josephine in 1984 are analyzed in this paper. In addition, wind-driven currents at several XCP's during Josephine are simulated using a one-dimensional ocean current model.

I. INTRODUCTION

An accurate quantitative determination of design environmental conditions is of great importance for offshore design consideration in oil and gas exploration and production, because of the high costs associated with the construction of deepwater offshore structures. For design consideration in such areas as the Gulf of Mexico, offshore China, and the northwest shelf off Australia, tropical cyclone generated forces in water column have been conventionally used as the major factor. Normally, forces generated by the maximum wave (extreme wave condition) and forces generated by the maximum possible wind-driven currents (extreme current condition) at a particular area are calculated for design consideration. The design criteria resulting from such a consideration may be overly conservative since the extreme wave and extreme current generally do not occur at the same time, at the same location, or in the same direction. Due to difficulties in measuring currents during a storm, however, little is known about the concurrent wind-driven current profiles in the vicinity of the maximum wave zone or the time lag between the maximum wave and maximum current conditions at a given site.

Measured currents at a site may be composed of currents driven by tide, wind, density gradient due to temperature and/or salinity distribution, gravity wave and localized circulation patterns such as internal waves and inertial currents. During a severe storm, the wind-driven

[1] Coastal and Oceanographic Engineering Dept., University of Florida, Gainesville, FL 32611
[2] Standard Oil Production Company, Dallas, Texas

currents become dominant over the other currents. Although a number of current models have been and are being used to calculate the wind-driven currents during severe storms, there is insufficient data available to validate these models. Based on extremely scarce data, however, Gordon (1982) claimed that currents in the ocean surface mixed layer (SML) are very uniform and only "slab model" can represent the current profiles in severe storms.

With the recent development of Air-deployed eXpendable Current Profiler, (Feeney, et al., 1985) or AXCP, "snapshots" of detailed ocean current and temperature profiles within storms can now be measured. It is thus possible to perform a systematic observation and analysis of wind- and wave-induced ocean currents at the ocean surface, surface mixed layer and thermocline. In addition, the wind-driven currents can be used for validation of ocean current models. In 1984, current profiles were measured via the systematic deployment of 31 AXCP's during two hurricanes—Hurricane Norbert in the eastern Pacific, and Hurricane Josephine in the western Atlantic.

This paper presents and discusses, from the point of view of practical engineering application, some ocean current and temperature profiles obtained via AXCP's in Hurricane Josephine during October, 1984. In addition, this paper presents a simulation of the wind-driven currents at several locations in Hurricane Josephine by means of a one-dimensional ocean current model (OCM1D) developed by Sheng (1984a and 1985). The results and understanding obtained from systematic studies such as this one will undoubtedly lead to the ultimate improvement of design criteria for offshore structures.

II. THE OBSERVATION PROGRAM

XCP and AXCP

The expendable current profiler (XCP) was originally developed by Dr. Thomas B. Sanford of Horizon Marine, Inc. It is a free-falling magnetic current meter which can be deployed from either a ship or an aircraft (AXCP). Figure 1 shows the major components involved in the XCP and AXCP deployment (Haustein and Feeney, 1985).

The ocean can be considered as many individual vertical layers with different electric fields which arise because of a process known as motional induction, i.e., electric current is generated as seawater flows through the geomagnetic field of the earth. The AXCP, as it falls through the water column, measures the electric current generated in each of the individual vertical layers via the recorded voltage (in nanovolts) between two horizontally spaced electrodes 5 cm apart. The measured electric currents at all layers yield a vertical profile of relative water velocities or "shears". A compass coil within the spin-stabilized probe measures the direction of current once per revolution as the probe falls with a 16 Hz rotation rate. A continuous temperature profile is measured by a thermistor located within the probe. The regular AXCP has a fall velocity of about 5m/sec and measures the current speed, direction and temperature to a depth of 1500 m. The slow-fall XCP has a fall velocity of about 2m/sec and a 200m depth capacity.

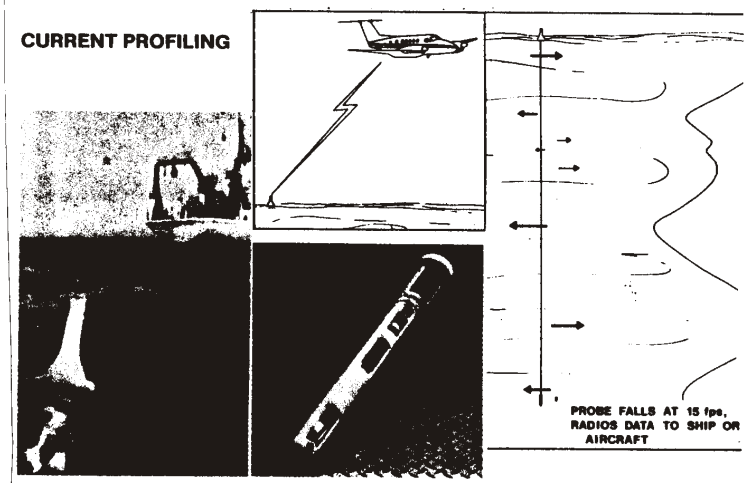

Figure 1 Current profiling using the XCP and AXCP. LEFT: Ship deployment showing attached float bag containing a radio antenna which transmits data back to the ship. CENTER TOP: Aircraft deployment. CENTER BOTTOM: The current profiler, contained within the probe housing. RIGHT: Continuous ocean current profile produced by the descending probe.

Forty seconds after the XCP lands on the water surface, the probe is launched through the bottom of the buoy. Signals measured by the electrodes, compass coils, and thermistor are transmitted from the probe to the surface buoy via a 1500-m or 200-m wire link. The data is then transmitted from the surface buoy, via the RF link, to processing or recording equipment on board a ship or aircraft. However, because the extremely strong winds during storms, the XCP's generally have a rather high failure rate of about 50%.

Ocean Response to a Hurricane

The observation program, "Ocean Response to a Hurricane", was a joint industry program involving nine U.S. oil companies (including Standard Oil, Mobil, Shell, etc.), NOAA's Hurricane Research Division and Office of Aircraft Operations, and Horizon Marine, Inc. (Feeney, et al., 1985). The program was the first systematic effort to measure ocean currents and temperature perturbations under severe meteorological conditions. A total of 31 AXCP's were systematically deployed during two hurricanes in 1984: Hurricane Norbert near Baja Peninsula in the eastern Pacific during September 23-24, and Hurricane Josephine near western Atlantic during October 10-11. While Norbert is relatively stronger, this paper concentrates on the slightly weaker Hurricane Josephine.

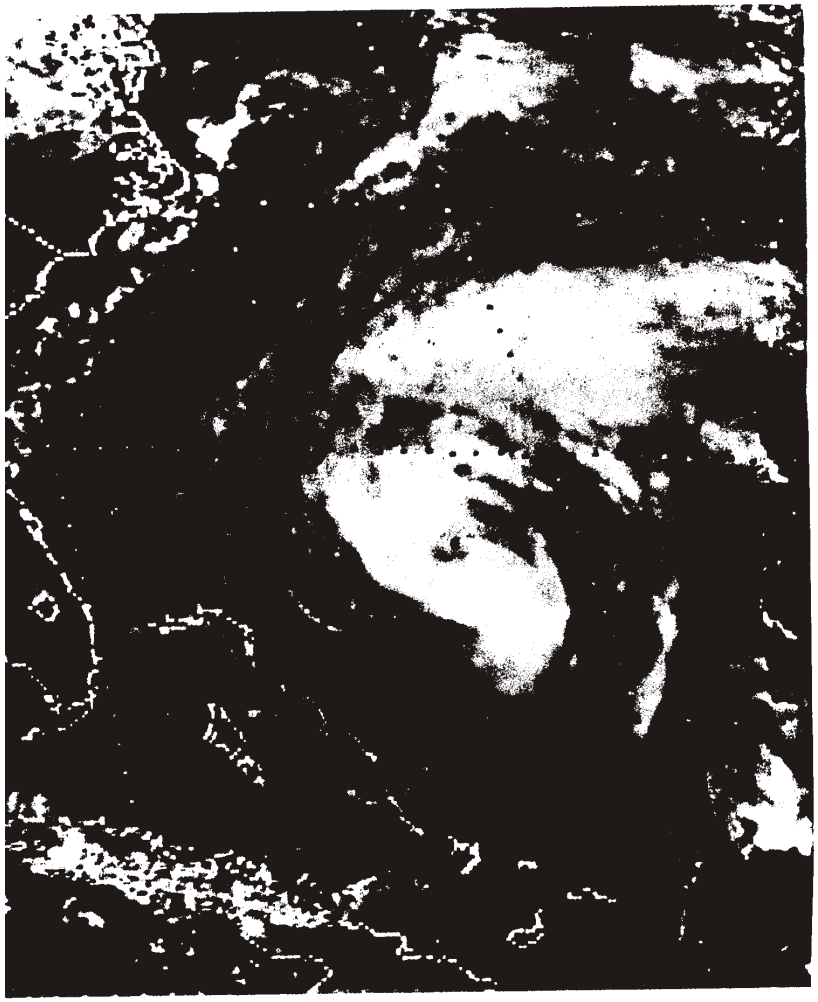

Figure 2 Hurricane Josephine as seen from satellite.

Hurricane Josephine

Flight through Josephine was executed on October 11, 1984, one day after Josephine attained hurricane strength. At that time, Josephine's eye was located near 25.5° N and 72° W with a moderate maximum surface wind of 75 knots and a barometric pressure of about 970 mb. The storm as shown in Figure 2 is located approximately 250 n miles northeast of the Bahama* Islands, drifting slowly northward, over waters of approximately 4000 m deep. The survey was conducted with a total of 31 AXCP's which include 17 regular AXCP's with a 1500 m depth capacity and 14 slow-fall AXCP's with a 200 m depth capacity.

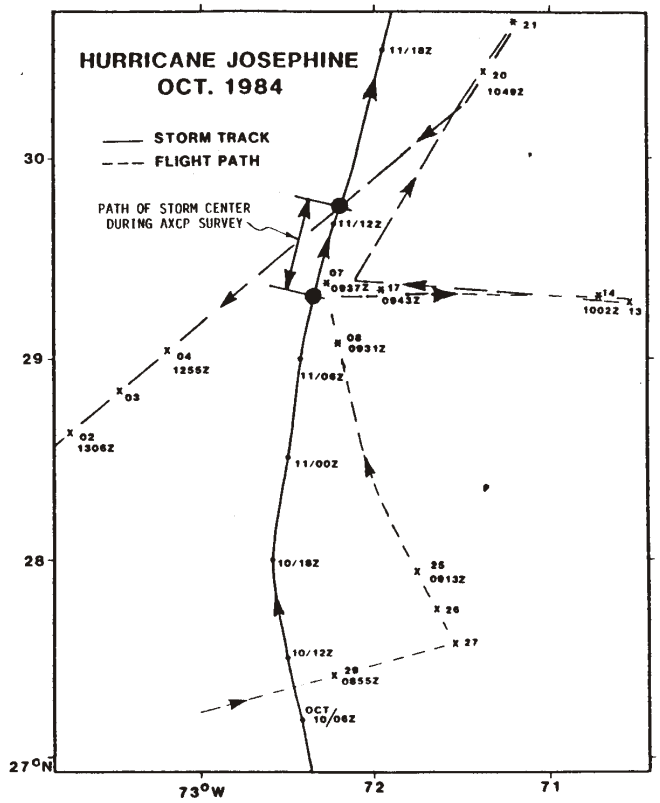

Figure 3 Storm track and AXCP flight path during Hurricane Josephine on October 10-11, 1984.

The flight area of the AXCP survey is shown in Figure 3, where the solid line starting from the south represents the storm track (distance between two adjacent dots represents a 6-hour interval) and the dashed line indicates the flight path between 8:45 AM (Zulu time) and 13:06 PM on October 11, 1984. The highlighted portion in Figure 3 represents the locations of storm center during the flight survey period. During that time, the forward speed of the hurricane was approximately 7 kts and the radius of maximum wind (R) was approximately 35 n miles. The survey covered an area more than 200 n miles (3 degrees) squared. Although a total of 31 AXCP's were deployed, only 50% of the data were usable. Locations with usable XCP data are indicated by the x's in Figure 3. 5 XCP's (XCP07, XCP08, XCP14, XCP17, and XCP21) are of special interest in this paper and are marked by the *'s in Figure 3.

III. XCP DATA DURING HURRICANE JOSEPHINE

All the XCP's were deployed to the right of Hurricane Josephine where the storm effect on current is stronger and where the Gulf Stream has negligible effect, thus allowing easier separation of wind- and wave-induced currents from the background current. Some data are presented in the following.

Current and Temperature Data at XCP17

XCP17 is located at approximately 0.7 R to the east of the storm eye. At the time of the survey, surface wind at XCP17 is about 24 kts toward the north. Several hours before the survey, however, wind exceeded 50 kts at all the XCP's of special interest.

Figure 4 shows the measured current speed, direction, and temperature at XCP17 from surface to 250 m depth. The profiles are plotted from data averaged over every 3 or 4 meters, or approximately 20 raw data points. The current speed (solid line) exceeds 1 m/sec at the surface and decays to about 20 cm/sec below 100 m depth, while the current direction (dotted line) changed form nearly 45° (towards northeast) at surface to about 180° (towards south) below 100 m depth. The effect of surface gravity wave, as is evidenced by the oscillatory velocity profile, is present even below 100 m depth.

Since our primary interest is the wind-driven current, a filtering procedure can be designed to remove the wave-induced orbital velocity from the signal. The filtering procedure makes use of the calculated wave period and the fact that amplitudes of the wave-induced signal decays exponentially with depth. The filtered current speed and direction as shown in Figure 4 are rather smooth and represent the wind-driven current, which will be used for validation of ocean current model. It should be noted that although wave signal can be found even at 100 m depth, the vertical shear associated with the wave orbital velocity is generally rather weak compared to that due to the wind-driven or density-driven currents. Hence, removing the wave-induced signal from current data will have little effect on turbulent mixing in the surface mixed layer.

Figure 4 also shows a thermocline between 70 m and 90 m depths. It is clear that although the temperature is rather uniform within the SML, current profile looks hardly like a "slab". In fact, significant shear

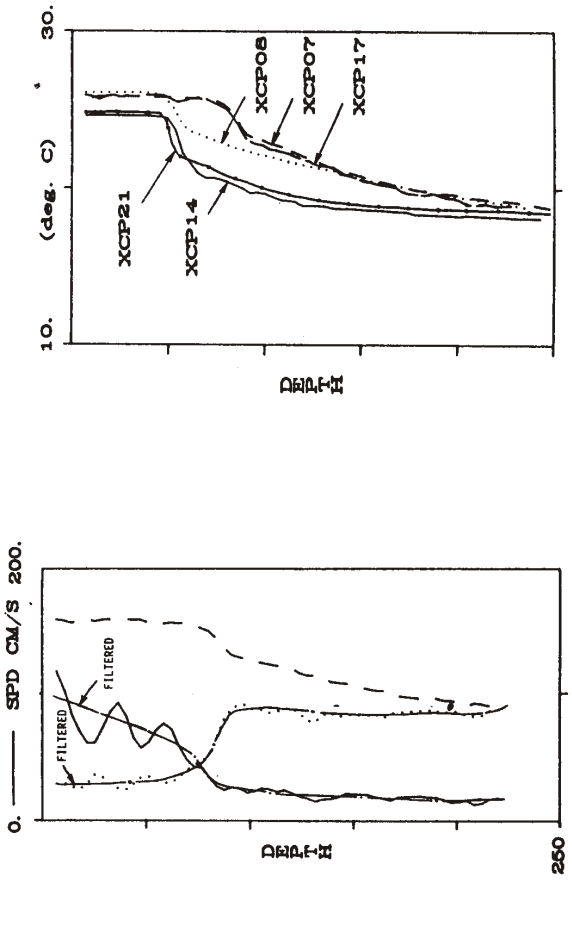

Figure 4 Current speed, current direction, and temperature measured by XCP17 during Hurricane Josephine.

Figure 5 Temperature profiles measured by XCP07, XCP08, XCP14, XCP17 and XCP21.

appears to be present in the mixed layer. It is also noted that the current profile does not quite resemble the classical Ekman layer. Except near the thermocline, little change in current direction is detected.

Temperature Data at XCP07, XCP08, XCP14, XCP17, and XCP21

Temperature profiles at the 5 XCP's are shown in Figure 5. At the three stations within R from storm center (XCP07, XCP08 and XCP17), temperature profiles within the SML are very similar, with XCP07 and XCP17 having almost identical profiles throughout the 250 m depth. At XCP14 and XCP21, more than 2R away from the storm eye, the temperature profiles are similar and relatively undisturbed by the hurricane. The SML temperature at these two XCP's is colder than that at the other three XCP's.

Thermocline at the XCP14 and XCP21 is found at 50 m depth. At XCP07 and XCP17, where winds are 1 kt and 24 kts respectively, but were much stronger several hours before, the thermoclines are found at 80 m depth. At XCP08, where the storm center has passed by about 4 hours ago and the wind is 9 kts, the thermocline is at 50 m depth.

The above data indicate that a time lag on the order of a few hours exists between the occurrences of peak wind and maximum thermocline deepening. As the storm center approaches a location, wind gradually decreases from peak wind to negligible wind when the eye arrives. When the storm center reaches the location, although the wind has decreased substantially, the thermocline continues to be deepened by wind-induced mixing generated during previous hours. At the same time, the positive wind stress curl may produce a positive vertical velocity which tends to move the thermocline upward. This so-called "Ekman suction", however, may also lag behind the arrival of storm center. In addition, lateral pressure gradient within the maximum radius R of the storm eye may also cause geostrophic currents and contribute to the mixing and migration of thermocline. However, the exact manner in which these competing mechanisms operate is not yet clearly understood.

Current Data at XCP07, XCP08, XCP14, and XCP17

Figure 6 shows the unfiltered current and temperature profiles at the 4 XCP's. If one visually removes the wave-induced components from Figure 6, it is apparent that the filtered current profiles in the SML are rather similar. The current decreases gradually with depth in the SML without any resemblance to the so-called "slab".

Current speed in the SML becomes increasingly stronger from XCP08 (< 50 cm/sec) to XCP07 (< 75 cm/sec) to XCP17 (< 1 m/sec). Current direction within much of the SML appears to be at approximately 45° to the right of the wind. Although the wind at XCP14 is the strongest (54 kts) among the 4 XCP's, the wind-driven current is only about 60 to 70 cm/sec. Velocity gradients within the thermoclines are quite different, apparently because of the difference in thermocline shapes. Below the thermocline, there appears to be an anticyclonic gyre around the storm center. Although this could be related to the geostrophic current induced by the pressure gradient, it is unclear as to how

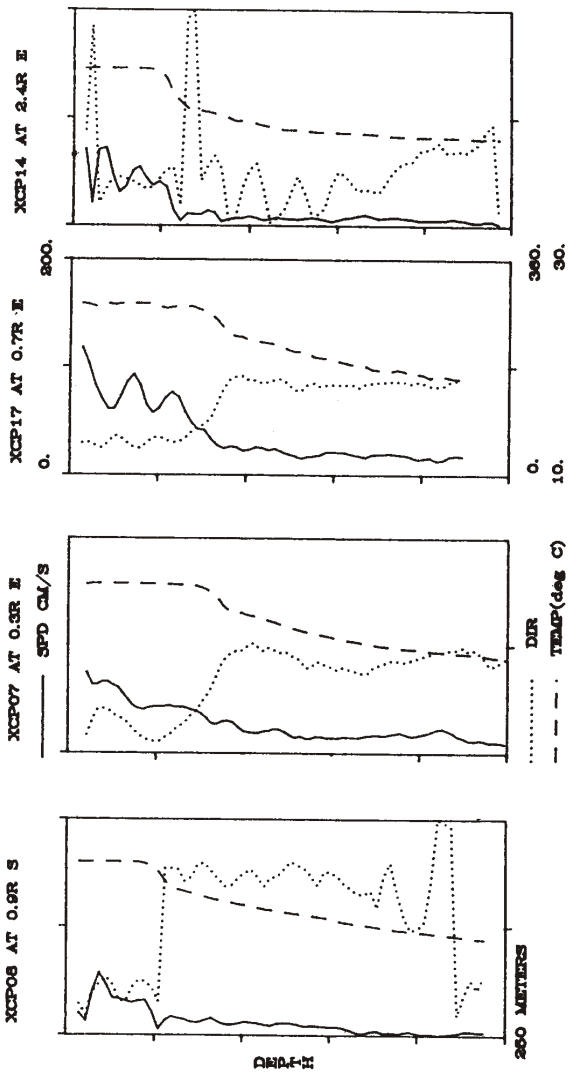

Figure 6 Measured current speed, current direction and temperature at XCP07, XCP08, XCP14 and XCP17.

sea surface slope, atmospheric pressure gradient and density gradient are known (either measured or computed) and specified as input to the model. However, these non-local terms and the solar radiation term in Eq. (3) are not used in the present study.

Turbulent fluxes $\overline{u'w'}$, $\overline{v'w'}$, $\overline{w'T'}$ and $\overline{w'S'}$ are modeled with the so-called "super-equilibrium" version of a second-order closure model of turbulent transport (Sheng, 1984a). The general equations are given in terms of $\overline{u_i'u_j'}$, $\overline{u_i'\rho'}$, and $\overline{\rho'\rho'}$ in tensor notations:

$$0 = -\overline{u_i'u_k'}\frac{\partial u_j}{\partial x_k} - \overline{u_j'u_k'}\frac{\partial u_i}{\partial x_k} - g_i\frac{\overline{u_j'\rho'}}{\rho_o} - g_j\frac{\overline{u_i'\rho'}}{\rho_o}$$
$$- 2E_{ik\ell}\Omega_k\overline{u_\ell'u_j'} - 2E_{jk\ell}\Omega_\ell\overline{u_k'u_i'} \qquad (6)$$
$$- \frac{q}{\Lambda}\left(\overline{u_i'u_j'} - \delta_{ij}\frac{q^2}{3}\right) - \delta_{ij}\frac{q^3}{12\Lambda}$$

$$0 = -\overline{u_i'u_j'}\frac{\partial \rho}{\partial x_j} - \overline{u_j'\rho'}\frac{\partial u_i}{\partial x_j} - \frac{g_i\overline{\rho'\rho'}}{\rho_o}$$
$$- 2E_{ijk}\Omega_j\overline{u_k'\rho'} - 0.75\,q\frac{\overline{u_i'\rho'}}{\Lambda} \qquad (7)$$

$$0 = -2\overline{u_j'\rho'}\frac{\partial \rho}{\partial x_j} - \frac{0.45\,q\,\overline{\rho'\rho'}}{\Lambda} \qquad (8)$$

In addition to the above equations, Λ is computed from three integral constraints, i.e., Λ is bounded by (1) a slope of 0.65, (2) q/Λ, where q is the total turbulent velocity and N is the Brunt-Vaisala frequency, and (3) a fraction of the spread of turbulence. This model was able to successfully simulate the laboratory wind-driven currents (Sheng, 1984a) storm generated currents on continental shelf (Sheng and Szabo, 1986).

A 60 hour model simulation, starting from 60 hours prior to the time of the survey, was performed at all XCP's by assuming XCP21's temperature profile and zero velocity as initial data. The results at XCP17 between hour 42 and hour 57, with a 3-hour interval, are shown in Figure 7. Currents in the SML grow steadily with time in spite of the decrease in wind speed during the last 2 hours. During the 15 hour period, current direction changed from towards NNW to towards NNE as the wind shifted from E to SSE. Thermocline was deepened during the last 6 hours.

Model Results at XCP07, XCP08, XCP14, and XCP17

Model results at the end of 60 hour simulation are shown in Figure 8 for XCP07, XCP08, XCP14 and ACP17. Filtered data are also shown on the same figure. In general, the agreement between model results and data are quite good. The best agreement is at XCP14 which

is at 2.4 times the maximum wind radius from the storm center and hence is not much affected by pressure gradient within the storm center. The current direction at all the XCP's appears to be correctly simulated although current speed at XCP08 seems underestimated. The discrepancy between model results and data at the 3 XCP's within the storm center can be attributed to the following 3 possibilities: (1) uncertainty in the initial condition, (2) pressure gradient not included in the present model simulation, and (3) possible vertical water movement associated with the curl of wind stress was not included in the model simulation.

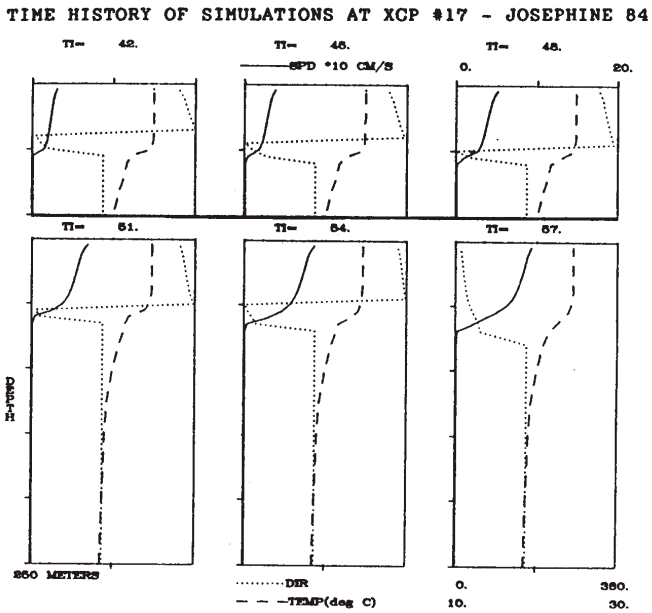

Figure 7 Model simulation of current and temperature at XCP17 during the six 3-hour intervals prior to the arrival of storm center.

V. CONCLUSIONS

During Hurricane Josephine in 1984, a systematic survey of ocean current and temperature within the top 250 m of ocean water was conducted by a joint industry program via the deployment of 31 AXCP's. This paper presents an analysis of the detailed data, which is available

exactly the pressure gradient and the wind stress interact to cause transient circulation in a hurricane. However, at XCP08, the greater difference (~180°) in current directions below and above the thermocline is consistent with the fact that pressure gradient at XCP08 is stronger than the other XCP's.

TABLE 1

SITE ID: XCP 17 0943Z LOCATION - 29.33N 71.07W
HURRICANE JOSEPHINE (OCT. 7-12,1984)

DATE	TIME	WIND DIR (DEG)	WIND SPEED MPS	WIND SPEED (KT)	WAVE H(SIG) (M)	WAVE H(SIG) (FT)	WAVE H(MAX) (M)	WAVE H(MAX) (FT)	WAVE Tpeak SEC	STORM DIST (NM)	STORM AZM DEG	PRES MBAR
	1300	68	9.6	19	2.13	7.0	4.40	14.4	5.0	224	3	1009
	1400	69	10.2	20	2.57	7.8	4.89	16.1	5.4	214	4	1009
	1500	69	10.9	21	2.62	8.6	5.40	17.7	5.9	203	4	1009
	1600	70	11.9	23	2.96	9.7	6.10	20.0	6.5	192	5	1008
	1700	70	12.5	24	3.32	10.9	6.84	22.5	6.9	183	5	1008
	1800	71	13.4	26	3.68	12.1	7.59	24.9	7.3	175	6	1007
	1900	71	14.1	27	3.98	13.1	8.21	26.9	7.7	168	6	1007
	2000	72	14.7	28	4.22	13.8	8.71	28.6	8.0	163	7	1007
	2100	72	15.1	29	4.38	14.4	9.04	29.7	8.2	159	7	1007
	2200	73	15.4	30	4.53	14.9	9.35	30.7	8.5	155	8	1006
	2300	73	15.8	31	4.69	15.4	9.67	31.7	8.5	151	8	1006
10 10 84	000	74	16.0	31	4.83	15.8	9.97	32.7	8.6	147	9	1006
	100	74	16.3	32	4.97	16.3	10.25	33.6	8.7	144	9	1006
	200	74	16.6	32	5.10	16.7	10.53	34.6	8.9	140	9	1006
	300	75	17.0	33	5.25	17.2	10.84	35.6	9.0	136	10	1005
	400	75	17.5	34	5.42	17.8	11.18	36.7	9.1	132	10	1005
	500	75	17.9	35	5.57	18.3	11.49	37.7	9.3	128	10	1005
	600	76	18.3	36	5.70	18.7	11.76	38.6	9.4	125	11	1005
	700	76	18.5	36	5.73	18.8	11.83	38.8	9.5	123	11	1005
	800	77	18.7	36	5.75	18.9	11.87	38.9	9.5	120	12	1005
	900	77	18.8	36	5.75	18.9	11.87	38.9	9.5	119	12	1005
	1000	78	18.8	37	5.75	18.9	11.86	38.9	9.5	117	13	1005
	1100	78	18.9	37	5.76	18.9	11.88	39.0	9.5	115	14	1005
	1200	79	18.8	36	5.76	18.9	11.88	39.0	9.5	112	14	1005
	1300	80	19.4	38	5.96	19.6	12.30	40.3	9.5	109	15	1004
	1400	81	20.0	39	6.17	20.2	12.74	41.8	9.7	106	16	1004
	1500	82	20.7	40	6.40	21.0	13.21	43.3	9.9	102	17	1003
	1600	84	21.2	41	6.62	21.7	13.65	44.8	10.0	99	19	1003
	1700	85	21.9	42	6.84	22.4	14.12	46.3	10.2	95	20	1002
	1800	86	22.5	44	7.07	23.2	14.60	47.9	10.4	91	21	1001
	1900	87	23.1	45	7.26	23.8	14.98	49.1	10.5	87	22	1001
	2000	88	23.8	46	7.44	24.4	15.35	50.4	10.7	82	23	1000
	2100	88	24.6	48	7.65	25.1	15.79	51.8	10.8	77	23	1000
	2200	89	25.4	49	7.87	25.8	16.22	53.2	11.0	72	24	999
	2300	90	26.3	51	8.09	26.5	16.59	54.4	11.1	67	25	998
10 11 84	000	92	26.9	52	8.29	27.2	16.93	55.5	11.3	63	27	997
	100	94	27.8	54	8.47	27.8	17.19	56.4	11.4	58	29	996
	200	96	28.7	56	8.58	28.1	17.33	56.8	11.5	54	31	995
	300	99	29.5	57	8.68	28.5	17.44	57.2	11.6	49	34	994
	400	103	30.1	59	8.76	28.8	17.42	57.2	11.7	45	36	993
	500	107	30.8	60	8.85	29.0	17.38	57.0	11.7	41	42	991
	600	112	28.6	56	8.56	28.1	16.70	54.8	10.5	36	47	989
	700	118	26.9	52	7.61	25.0	14.61	47.9	10.5	31	53	987
	800	127	21.5	42	6.56	21.5	12.47	40.9	9.4	25	62	983
	900	141	12.4	24	5.52	18.1	10.33	33.9	9.5	20	76	980
	1000	162	7.5	15	4.88	16.0	9.07	29.7	8.5	17	97	977
	1100	188	7.8	15	4.86	15.9	8.98	29.5	8.5	17	123	976
	1200	213	13.1	26	5.65	18.5	10.64	34.9	7.6	20	148	977

II. MODEL SIMULATION OF WIND-DRIVEN CURRENTS IN JOSEPHINE

Wind and Wave Hindcasting

Before simulating the wind-driven currents, the wind and wave field were hindcasted by means of a modified Bretschneider method (1972). With such input values as storm track, central pressure, maximum wind radius, R, maximum wind at R, and ambient flows, the model yields the wind and wave conditions. As an example, the hindcast wind and wave data at XCP17 during a 48 hour period prior to the arrival of Josephine are shown in Table 1. At 5:00 AM on October 11, while the storm center is still 41 n m (nautical miles) from XCP17, the wind speed peaked to 60 kts and the significant wave height peaked to 29 feet with a peak period of 11.7 sec. Four hours later at 9:00 AM, the condition has fallen to 24 kts wind speed, 18 feet wave height, and 9.5 sec wave period.

The time-dependent wind fields at all the XCP locations were saved in computer storage and used for simulation of wind-driven currents. Although the pressure was also computed by the hindcast model, it was not used for the present model simulation of wind-driven currents.

A One-Dimensional Ocean Current Model: OCM1D

Sheng (1984a and 1985) developed the OCM1D based on the following mean equations of motion:

$$\frac{\partial u}{\partial t} = fv - \underline{\frac{\partial \overline{u'w'}}{\partial z} - g\frac{\partial \zeta}{\partial x} - \frac{1}{\rho_o}\frac{\partial P_a}{\partial x} + \frac{g}{\rho_o}\int_o^z \frac{\partial \rho}{\partial x}\,dz} \tag{1}$$

$$\frac{\partial v}{\partial t} = -fu - \underline{\frac{\partial \overline{v'w'}}{\partial z} - g\frac{\partial \zeta}{\partial y} - \frac{1}{\rho_o}\frac{\partial P_a}{\partial y} + \frac{g}{\rho_o}\int_o^z \frac{\partial \rho}{\partial y}\,dz} \tag{2}$$

$$\frac{\partial T}{\partial t} = -\frac{\partial \overline{w'T'}}{\partial z} + \underline{\eta(1 - A_s)\frac{\phi_o}{\rho_o C_p}\exp(-\eta z)} \tag{3}$$

$$\frac{\partial S}{\partial t} = -\frac{\partial \overline{w'S'}}{\partial z} \tag{4}$$

$$\rho = \rho(T,S) \tag{5}$$

where (u,v) are the horizontal velocities in (x,y) directions, T is temperature, S is salinity, z is the vertical coordinate pointing upward from z = 0 at the undisturbed ocean surface, ζ is surface displacement, ρ_o is reference density, P_a is atmospheric pressure, ρ is density, (u',v',w') are turbulent fluctuating velocities in (x, y, z) directions, T' and S' are fluctuating temperature and salinity, η is extinction coefficient of solar radiation, A_s is sea surface absorption coefficient, and ϕ_o is solar raditation flux at sea surface. The underlined terms in Eqs. (1) and (2) are non-local terms which can be evaluated if

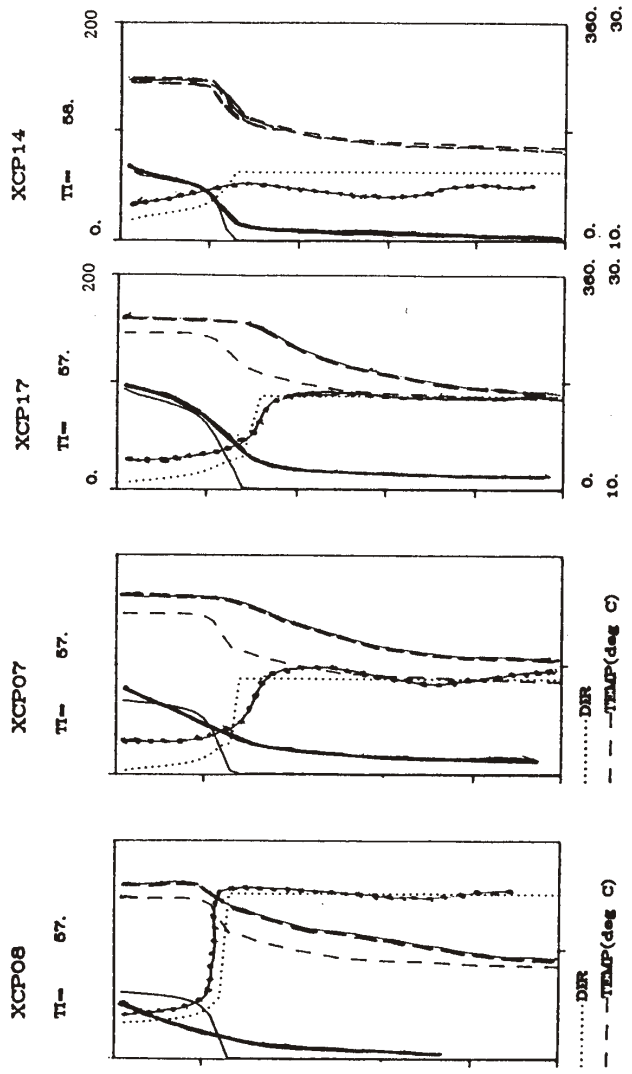

Figure 8. Model simulated and measured current and temperature at XCP07, XCP08, XCP14, and XCP17. Darker lines indicate measured data.

for the first time, and found the data of significant value for further understanding of ocean mixed layer dynamics and for improvement of offshore design criteria.

Model simulation of storm-generated currents at several XCP's was carried out by using the 1-D Ocean Current Model (OCM1D). The results generally are in reasonable agreement with data. It is interesting to note that both XCP data and model results showed significant shear within the surface mixed layer and no "slab"-like current profile was found. Discrepancy between model results and data is attributed to uncertainty in initial condition and neglect of pressure gradient and Ekman-suction in model simulation.

VI. ACKNOWLEDGEMENTS

The first author wishes to acknowledge the support of Standard Oil Production Company and Mobil Research and Development Corporation for the development of the 1-D ocean current model. Sherman Chiu served as the technical monitor for SOPO while David Szabo and Max Sheppard served as technical monitors for MRDC.

VII. REFERENCES

Bretschneider, C. L., 1972: "A Non-Dimensional Stationary Hurricane Wave Model", OTC paper 1517.

Feeney, J. W., T. B. Sanford, and J.R. Haustein, 1985: "Observing Hurricane-Driven Waves and Currents", OTC paper 4934.

Gordon,R. L., 1982: "Coastal Ocean Current Response to Storm Winds", JGR, 87, C3, p. 1939.

Haustein J. R. and J. W. Feeney, 1985: "Gulf of Mexico Deep Water Current Studies for Offshore Oil Exploration and Production", Oceans 85, pp. 1062-1070.

Sheng, Y. P., 1984a: "A Turbulent Transport Model of Coastal Processes", Proc 19th Intl. Conf. Coastal Eng., ASCE, pp. 2380-2396.

Sheng Y. P., 1984b: "A One-Dimensional Ocean Current Model (OCM1D)", A.R.A.P. Report No. 523, prepared for Mobil Research and Development Corporation, A.R.A.P., Princeton, NJ.

Sheng, Y. P., 1985: " A New One-Dimensional Model of Ocean Current", A.R.A.P. Report Prepared for Standard Oil Production Company, Princeton, NJ.

Sheng Y. P. and D. Szabo, 1986: "Validation of Current Model OCM1D in Storm Conditions", A.R.A.P. Report No. 580, Prepared for Mobil Research and Development Corporation, A.R.A.P., Princeton, NJ.